VII. CONCLUSIONS

Complete design formulas have been obtained for waveguide single-sided filters where only one passband and one stopband are required. It has been shown, that a significant reduction in the number of cavities needed to meet this type of specification can be obtained over conventional techniques. Furthermore, the structure is physically no more complicated than the conventional waveguide bandstop filter, the only difference being irregular spacings of the stubs.

The three classes of filters which achieve quasi low-pass or quasi high-pass responses have been discussed in detail and simulated on a digital computer. Finally, experimental results on a fifth-degree X-band filter have been presented for the three quarter wave coupled case with and without compensating capacitive discontinuities showing very close agreement to theoretical predictions.

REFERENCES

[1] S. B. Cohn, "Direct-coupled-resonator filters," *Proc. IRE*, vol. 45, pp. 187–196, Feb. 1957.
[2] G. L. Matthaei, L. Young, and E. M. T. Jones, *Microwave Filters, Impedance-Matching and Coupling Structures*. New York: McGraw-Hill, 1964.
[3] J. D. Rhodes, "Waveguide bandstop elliptic function filters," *IEEE Trans. Microwave Theory Tech.*, vol. MTT-20, pp. 715–718, Nov. 1972.
[4] ——, "Explicit formulas for element values in elliptic function prototype networks," *IEEE Trans. Circuit Theory*, vol. CT-18, pp. 264–276, Mar. 1971.

Temperature-Stabilized 1.7-GHz Broad-Band Lumped-Element Circulator

HIDEHIKO KATOH

***Abstract*—A new construction technique for broad-banding and temperature stabilization of a lumped-element circulator is presented to obtain a compact circulator for practical usage. By using a new integrated wide-banding network consisting of three series resonant circuits on the back of the junction substrate, 1.7-GHz double-tuned and triple-tuned broad-band circulators have been successfully developed. Fundamental junction parameters, such as an in-phase eigeninductance, parasitic capacitance, and nonreciprocal filling factor, have been investigated experimentally.**

A design theory for temperature compensation of a lumped-element circulator is also presented, and temperature compensation with bias magnetic field of postitive temperature coefficient has been applied to the 1.7-GHz broad-band circulators. As a result, 20-dB isolation bandwidths of more than 600 MHz (double-tuned type) and 950 MHz (triple-tuned type) have been obtained throughout the temperature range of $-10 \sim +60$°C.

I. INTRODUCTION

RECENT PROGRESS of thin-film lumped-element microwave integrated circuits (IC) for lower microwave frequencies has stimulated the need for miniaturized nonreciprocal circuits which are well adapted to the integrated circuits. By applying microwave IC technology, Knerr [1] realized an L-band lumped-element circulator [2], and afterwards achieved a 20-dB isolation relative bandwidth of more than 30 percent by inserting a capacitor between the junction base conductor and ground [3]. This broad-banding technique was recognized later [4] to be equivalent with the one proposed by Konishi and Hoshino [5], in which the in-phase eigenvalue is excited by an explicit resonant circuit. It is expected from the analysis by Konishi and Hoshino [5] that a broader bandwidth can be obtained if the resonant circuit is properly optimized. However, no experimental investigation in this respect has been made so far for frequency bands above 1.0 GHz.

Therefore, the main purpose of this paper is to propose a lumped-element circulator construction that uses a new type of integrated wide-banding network which is optimally adjusted and suitable for microwave frequencies. Experimental results on circulator junction in regard to its eigeninductances, parasitic reactances, and nonreciprocal filling factor [6] are also described.

In addition to broad-banding, temperature stabilization is important from the practical point of view. Konishi [2] discussed temperature dependence of lumped-element circulator characteristics, but the result is not applicable at least to below resonance circulators. Thus another purpose of this paper is to present a temperature stabilization technique. A design theory for temperature compensation of a lumped-element circulator is derived, and a stabilization method using a bias magnetic field of a positive temperature coefficient is proposed.

Manuscript received August 5, 1974; revised February 3, 1975.
The author is with the Central Research Laboratories, Nippon Electric Co., Ltd., Nakahara-ku, Kawasaki, Japan.

Based on the above results, 1.7-GHz-band temperature-stable wide-band lumped-element circulators have been developed, which have 20-dB isolation bandwidths of more than 600 MHz (double-tuned type) and 950 MHz (triple-tuned type) throughout the temperature range of $-10°C \sim +60°C$. These performances are superior to those previously reported [7].

II. BANDWIDTH BROADENING

A. Junction Parameters

An effective circuit for a double-tuned wide-band lumped-element circulator is shown in Fig. 1. In advance of the discussion on the wide-banding network, fundamental parameters of the junction part are specified. At first, parasitic capacitance and coupling strength for the usual junction structure will be discussed. Then, variation of the eigenvalue in a magnetic field will be formulated.

As shown in Fig. 1, the circulator junction consists of three short-circuited split microstrip inductors interwoven with one another. In an ideal case, the eigeninductances L_i and L_r for an in-phase and rotational excitation of the junction, respectively, are given [2], [8] as

$$L_i = 0, \qquad L_r = \tfrac{3}{2}L_0 \tag{1}$$

where L_0 is the inductance of a single split circulator. However, it has been recognized by the present author [9] that, in an actual circulator junction, there are gradual increases of L_r and L_0 against the signal frequency and a fairly large value of L_i.

The increase seems to be originated from the distributed parallel capacitance of junction inductors. Thus the values of the parallel inductance and capacitance have been separately obtained [10] by solving graphically several equations which are expressed as follows:

$$C = \frac{1}{\omega_i^2}\cdot\frac{1}{L} + \frac{B_i}{\omega_i} \tag{2}$$

where B_i is eigensusceptance measured at angular frequency ω_i and i is the number of frequencies.

As a result, the parasitic parallel capacitance has been proved to be due to crossover capacitance C_c and capacitance C_d distributed between the junction inductor and the base conductor. The latter is the same as the parasitic distributed capacitance of a single short-circuited microstrip inductor. Equivalent terminal capacitance C_p' for rotational excitation, which is approximately estimated [10] according to

$$C_p' = \tfrac{1}{3}C_d + 12C_c \tag{3}$$

serves as a part of the parallel capactance C_p in Fig. 1.

Typical relations between the inductances (L_r, L_0, and L_i) and the ferrite disk substrate thickness, thus obtained, are shown in Fig. 2. Since the part $(L_0 - L_i)$ of the inductance (L_0) participates in the coupling among split junction inductors, excitation ratio r of the rotating magnetic field should be expressed as follows:

$$r = \frac{L_r - L_i}{L_r}. \tag{4}$$

From Fig. 2, r is found to be usually about one-half.

In the operation of the circulator, the junction is loaded with ferrimagnetic material biased with an external magnetic field. The eigenvalue for rotational excitation is split into two for positive and negative excitation. Three inductive eigenimpedances of the junction, exclusive of parasitic capacitance, can be given as follows:

$$Z_{\pm} = j\omega L_r \mu_{\pm\text{eff}} \tag{5}$$

$$Z_i = j\omega L_i \mu_{i\text{eff}} \tag{6}$$

where $\mu_{\pm\text{eff}}$ and $\mu_{i\text{eff}}$ are effective permeabilities which work on an actual microstrip junction for the positive and negative rotational excitation and for the in-phase excitation, respectively.

In rotational excitation, only a rotating magnetic field in the ferrite substrate is concerned with nonreciprocal action of the circulator. Thus the nonreciprocal filling factor k_f is given as

$$k_f = q_m r \tag{7}$$

where q_m is the magnetic filling factor of a microstrip transmission line on a magnetic substrate [11]. The permeability for this rotating magnetic field is $\mu_{\pm}$, which

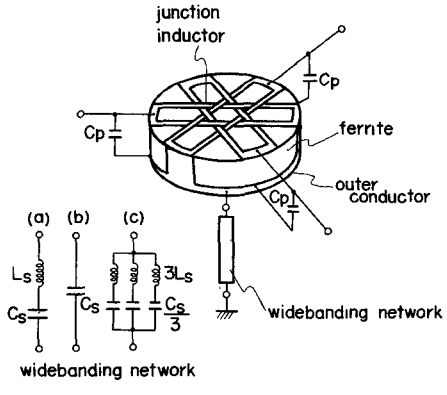

Fig. 1. Schematic circuit of a broad-band lumped-element circulator.

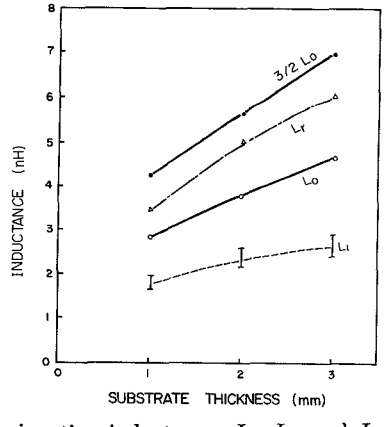

Fig. 2. Three junction inductances L_r, L_i, and L_0 versus a disk substrate thickness. The disk is 8 mm in diameter.

is given by the following prevalent formula:

$$\mu_{\pm} = 1 + \frac{P}{\sigma \mp 1} \tag{8}$$

$$P = \frac{|\gamma| 4\pi M_s}{\omega}, \qquad \sigma = \frac{|\gamma| H_i}{\omega} \tag{9}$$

$$H_i = H_{ex} - N_z \cdot 4\pi M_s \tag{10}$$

where γ is the gyromagnetic ratio, $4\pi M_s$ is a saturation magnetization, H_i is the internal magnetic field, H_{ex} is the external bias magnetic field, and N_z is a demagnetization factor of the substrate. Inductance L_i seems to be mainly a function of μ, which is given as

$$\mu = \frac{\mu_+ + \mu_-}{2} \tag{11}$$

because μ is the permeability for the wave on a stripline in magnetic material magnetized perpendicularly to the ground plane [12]. Thus three kinds of effective permeability are expressed as follows:

$$\mu_{\pm \mathrm{eff}} = k_f \mu_{\pm} + q_m(1 - r)\mu + 1 - q_m \tag{12}$$

$$\mu_{i\mathrm{eff}} = q_m \mu + 1 - q_m. \tag{13}$$

Fig. 3 shows experimental results of effective permeabilities $\mu_{\pm\mathrm{eff}}$ and $\mu_{i\mathrm{eff}}$, which have been obtained as $Z_{\pm}/j\omega L_r$ and $Z_i/j\omega L_i$, respectively. Comparing the experimental values with the calculated value of $\mu_{\pm}$ in (8), it is confirmed that the nonreciprocal filling factor k_f, which is given directly by ratio of $(\mu_{+\mathrm{eff}} - \mu_{-\mathrm{eff}})/(\mu_+ - \mu_-)$ [6], is less than a half in actual microstrip junction, corresponding to the presumed value by (4) and (7).

Usually, a bias magnetic field is applied so that σ should be almost zero, i.e., $\mu \approx 1$. In that case $\mu_{\pm\mathrm{eff}}$ becomes

$$\mu_{\pm\mathrm{eff}} = 1 + \frac{k_f P}{\sigma \mp 1}. \tag{14}$$

This is a Polder's expression (8) with effective saturation magnetization which is reduced by the factor k_f from the actual value. Therefore, the usual design procedure of a single-tuned circulator [2] is available, by introducing the effective saturation magnetization.

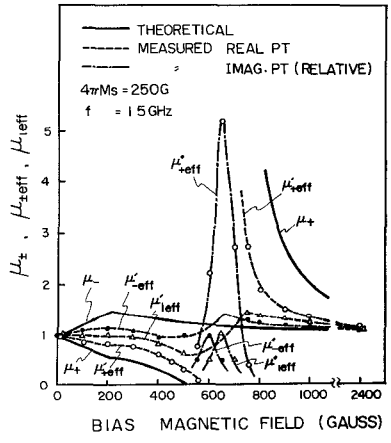

Fig. 3. Variation of effective permeabilities against bias magnetic field.

B. Broad-Banding by Excitation of In-Phase Eigenvalue

Effective circuits for wide-banding, as shown in Fig. 1(a) and (b), have been proposed previously [3], [5]. In case of the circuit in Fig. 1(a) [5], a series LC circuit is connected between the outer conductor and ground, so that the eigenvector of in-phase excitation exhibits the resonant variation corresponding to those due to the other two rotational excitations. It has also been shown by computer calculation [5] that there is an optimum value of m, which is given as

$$m = \frac{L_s}{C_p Z_0^2} \tag{15}$$

where Z_0 is the terminal impedance. In the actual construction of the circulator, connecting only one resonant circuit is apt to break the symmetry of the circulator at high frequencies such as microwave frequencies, unless a three-dimensional configuration is taken. However, this configuration is not appropriate for an MIC component.

In case of the circuit in Fig. 1(b) [3], a capacitor is connected so as to make use of the resonant behavior with the parasitic junction inductance L_i of an in-phase excitation [4]. However, it is impossible to optimize the resonant circuit, because inductance L_i is neither large enough for this purpose nor independent of junction inductance L_r for rotational excitation as was already shown in Fig. 2.

In order to obtain an integrated broad-banding circuit with good symmetry, a new wide-banding network is proposed, which consists of three parallel circuits as shown in Fig. 1(c). In Fig. 4, construction of an IC circulator using the wide-banding network of Fig. 1(c) is shown. Fig. 4(a), (b), and (c) show, respectively, the

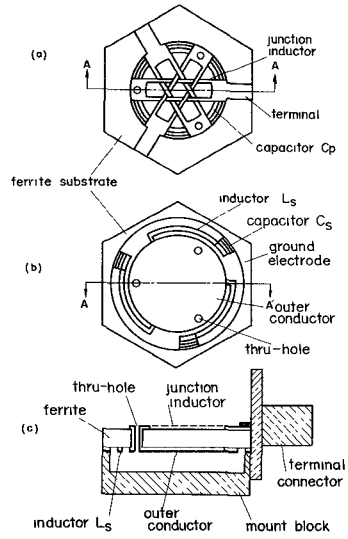

Fig. 4. Construction of an IC broad-band circulator. (a) Front side. (b) Back side. (c) AA' cross-sectional view of mounted substrate.

terminal and the junction circuit on the front side of the ferrite substrate, the wide-banding network on the back side, and a cross-sectional view of the mounted substrate. Three ends of junction inductors have been shorted with the outer conductor by through-hole plating.

It has been confirmed that even in the microwave frequency range of 1–2 GHz, this wide-banding circuit influences only the eigenvalue of the in-phase excitation, giving it the desired resonant characteristics as shown in Fig. 5. It is easy to optimize the parameter m by cutting apart shunt conductors of strip inductors or fingers of interdigital capacitors. Inductance L_i is considered as a part of the series resonant inductance L_s. Fig. 6 shows an actual variation of the input impedance of the circulator whose bandwidth is being broadened by the optimum adjustment.

An example of the 1.7-GHz band lumped-element circulator is shown in Fig. 7. The circulator case size (exclusive of connectors) is 18 mm by 19 mm, which is much smaller than that of conventional distributed-constant type in this frequency range. The ferrite substrate used in a 14 mm by 14 mm Ca–V garnet [13] whose saturation magnetization is about 400 G. Interdigital

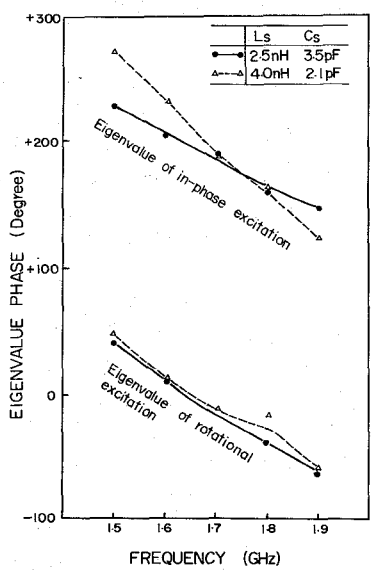

Fig. 5. Influence of the broad-banding series resonant circuit on circulator eigenvalues.

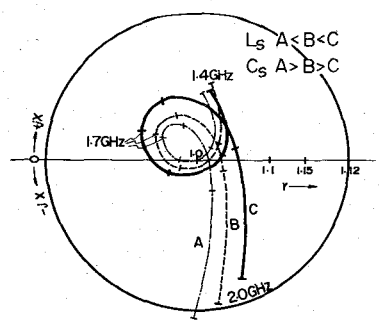

Fig. 6. Magnified Smith chart showing change of the input impedance due to wide-band optimization.

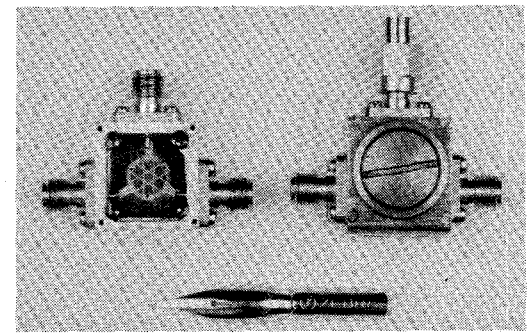

Fig. 7. Photograph of a broad-band lumped-element circulator with a dummy at one port (right) and with the magnetic circuit removed (left).

capacitors and strip inductors are made of evaporated Cr–Au and plated Au films prepared by means of conventional microwave IC technology, which includes the air-insulated beam-lead crossover process. The circulator has double-tuned characteristics, as will be shown later in Figs. 13 and 14. The best one showed, at room temperature, an isolation of more than 20 dB and an insertion loss of less than 0.85 dB (minimum 0.55 dB) over the frequency bandwidth of about 700 MHz centered at 1.67 GHz. The fractional bandwidth has been about 41 percent, while that of the single-tuned circulator before being wide-banded has been less than 10 percent.

C. Triple-Tuned Broad-Banding

It is seen from Fig. 6 that, at a proper standard plane, the input impedance of a double-tuned circulator with an in-phase eigenexcitation resonator is very similar to that of a two-stage bandpass filter as shown in Fig. 8. In fact, both input impedances have been proved to coincide rigorously on the basis of the narrow-band approximation [14]. Therefore, further broadening of bandwidth can be achieved by using the ordinary band-pass network synthesis theory.

Figs. 15 and 16 shown later are 1-GHz band characteristics of a triple-tuned circulator obtained by adding an appropriate one-stage series resonant circuit to each terminal of the double-tuned circulator. Thin-film series resonant circuits have been formed around the junction part shown in Fig. 5(a). The 20-dB isolation fractional bandwidth at room temperature has been widened to about 58 percent, which is competitive with that of the usual distributed constant circulators.

III. TEMPERATURE STABILIZATION

A. General Theory of Temperature Compensation

Temperature variation of saturation magnetization of the ferrite substrate causes variation of circulator characteristics. In this subsection, temperature compensation of an ideal single-tuned circulator is discussed.

There are five fundamental design parameters in a single-tuned circulator, i.e., frequency or angular frequency f or ω, saturation magnetization of ferrite $4\pi M_s$, external bias magnetic field H_{ex}, junction inductance for rotational

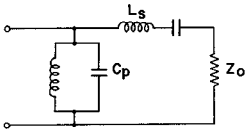

Fig. 8. Equivalent circuit of a two-stage band-pass filter.

excitation L_r, and parallel capacitance C_p. The following conditions apply to these parameters to realize a circulator [2]:

$$Y_+ = j\omega C_p + \frac{1}{j\omega\mu_+ L_r} = \pm j\frac{1}{\sqrt{3}Z_0} \tag{16}$$

$$Y_- = j\omega C_p + \frac{1}{j\omega\mu_- L_r} = \mp j\frac{1}{\sqrt{3}Z_0} \tag{17}$$

where upper and lower signs are for the case of above- and below-resonance circulator, respectively; the same expressions are used in the following. Y_+ and Y_- mean eigen-admittances of the positive and negative excitation, respectively.

Taking the sum and difference of (16) and (17), and substituting (8)–(10) into them with the assumption that the demagnetization factor N_z equals unity, circulator conditions become as follows:

$$\omega^2 - (|\gamma| H_{ex})^2 \pm \frac{\sqrt{3}Z_0}{L_r}|\gamma| 4\pi M_s = 0 \tag{18}$$

$$\omega^2 \pm \frac{|\gamma| H_{ex}}{\sqrt{3}C_p Z_0} - \frac{1}{C_p L_r} = 0. \tag{19}$$

It is also well known that the fractional bandwidth where backward transmission is kept within the amount of $|S''|$ is shown in the following equation [2]:

$$w = \frac{2|S''|}{[(\omega C_p Z_0)^2 + \frac{1}{4}]^{1/2}}. \tag{20}$$

The center frequency f of a circulator is set up at the design frequency. Junction inductance L_r does not change with temperature. Thus when $4\pi M_s$ varies with temperature, design parameters H_{ex} and C_p should vary so as to satisfy the conditions of a circulator. Keeping L_r and ω constant, and taking variation of H_{ex}, C_p and w in (18)–(20), the following relations are obtained:

$$\frac{dH_{ex}}{H_{ex}} = \pm\frac{\sqrt{3}P}{2lh^2}\cdot\frac{d(4\pi M_s)}{4\pi M_s} \tag{21}$$

$$\frac{dC_p}{C_p} = \frac{lh}{lh \mp \sqrt{3}}\cdot\frac{dH_{ex}}{H_{ex}} \tag{22}$$

$$\frac{dw}{w} = -\frac{4c^2}{4c^2+1}\cdot\frac{dC_p}{C_p} \tag{23}$$

where

$$h = \frac{|\gamma| H_{ex}}{\omega} = P + \sigma, \quad l = \frac{\omega L_r}{Z_0}, \quad c = \omega C_p Z_0. \tag{24}$$

From (18) and (19), l and c are given as follows:

$$l = \mp\frac{\sqrt{3}P}{1-h^2} \tag{25}$$

$$c = \mp\frac{Ph + 1 - h^2}{\sqrt{3}P}. \tag{26}$$

From the above expressions, the required quantity of H_{ex} and C_p to compensate for temperature variation of $4\pi M_s$ can be obtained definitely in the following form:

$$DH = \frac{dH_{ex}}{H_{ex}} \Big/ \frac{d(4\pi M_s)}{4\pi M_s} \tag{27}$$

$$DC = \frac{dC_p}{C_p} \Big/ \frac{d(4\pi M_s)}{4\pi M_s}. \tag{28}$$

The change of fractional bandwidth caused by this temperature compensation is also obtained in the following form:

$$DW = \frac{dw}{w} \Big/ \frac{d(4\pi M_s)}{4\pi M_s}. \tag{29}$$

The computed values of DH, DC, and DW are shown in Fig. 9, where the abscissa is the normalized internal magnetic field σ before being compensated for. Saturation magnetization usually decreases with an increase in temperature. It is seen from Fig. 9 that the external magnetic field should be adjusted toward the magnetic resonance field and the parallel capacitance should be increased with the rising temperature.

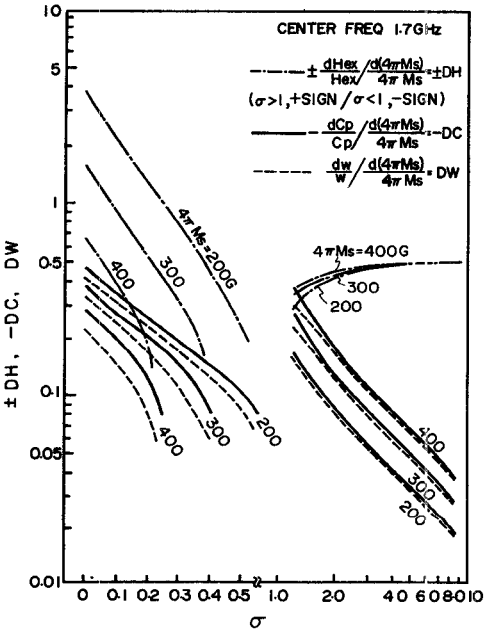

Fig. 9. Required compensation quantity and variation of fractional bandwidth in case of temperature compensation by bias magnetic field and parallel capacitance.

However, it is complicated and not always practical at present to use capacitors for compensation. Thus the shift of the center frequency of a circulator that is temperature-compensated only by H_{ex} has been investigated, keeping both L_r and C_p constant. If this shift is small enough, a substantial temperature compensation can be achieved.

Taking variation of H_{ex}, ω, and w in (18)–(20) under the condition of constant L_r and C_p, the following results are obtained:

$$\frac{dH_{ex}}{H_{ex}} = \frac{3P_c}{lh(1 \pm 2\sqrt{3}ch)} \cdot \frac{d(4\pi M_s)}{4\pi M_s} \tag{30}$$

$$\frac{d\omega}{\omega} = \frac{df}{f} = \mp \frac{h}{2\sqrt{3}c} \cdot \frac{dH_{ex}}{H_{ex}} \tag{31}$$

$$\frac{dw}{w} = -\frac{4c^2}{4c^2 + 1} \cdot \frac{df}{f}. \tag{32}$$

From the above relations and (24)–(26), the ratio DH of the adjusted amount of H_{ex} to the variation of $4\pi M_s$ is obtained. The change of center frequency DF, which is defined by

$$DF = \frac{df}{f} \Big/ \frac{d(4\pi M_s)}{4\pi M_s} \tag{33}$$

and the change of fractional bandwidth DW, can also be computed easily. An example of the results is illustrated in Fig. 10.

The results mentioned so far give us a general principle for designing the temperature-stable circulator. In actual application, a calculation should be carried out using $\mu_{\pm eff}$ instead of the ideal $\mu_{\pm}$, as represented in the previous section. However, Figs. 9 and 10 are available in the usual case where σ is set to be nearly zero, by replacing the parameter $4\pi M_s$ with the effective $4\pi M_s$ mentioned after (14). Consideration of another important case and a comparison with the previous theory [2] are discussed in the Appendix.

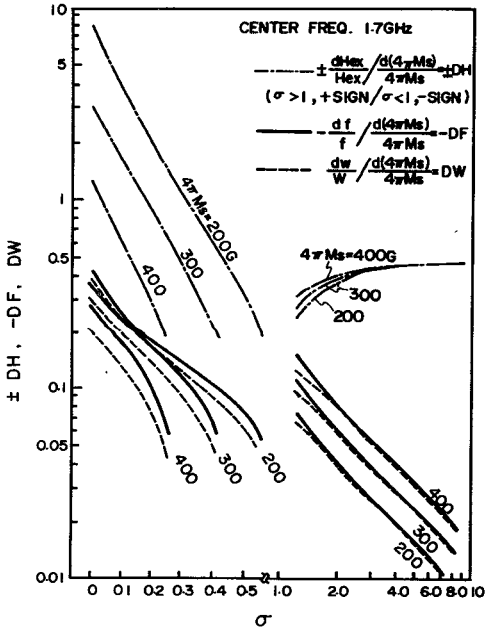

Fig. 10. Required compensation quantity and variation of center frequency and fractional bandwidth in case of temperature compensation only by bias magnetic field.

B. *Temperature-Stabilized* 1.7-GHz *Band Lumped-Element Circulator*

In the circulator discussed in Section II-B and C, Ca–V garnet of saturation magnetization of about 400 G has been used with an external bias magnetic field of 450 G. In this case, σ is about 0.1. The effective saturation magnetization seems to be about 200 G, assuming a nonreciprocal filling factor k_f of about 50 percent. As listed in Table I, the temperature coefficient of $4\pi M_s$ has been reduced to about -0.2 percent/°C without any increase of ΔH and tan δ_ϵ by improvement of the substrate material [15]. Then, as seen from Fig. 10, the circulator can be temperature-compensated by setting the temperature coefficient of the external magnetic field to about 0.8 percent/°C. The shift of the center frequency of the single-tuned circulator is predicted to be about 0.04 percent/°C.

A bias magnetic field with a positive temperature coefficient has been provided by loading a magnetic shunt alloy in parallel with a bias magnetic field, as shown in Fig. 11. Although the temperature coefficient of the magnetic field generated by a permanent magnet of AlNiCo alone is about -0.02 percent/°C, the magnetic field thus composed increases with temperature from -10°C to 60°C, as shown in Fig. 12. The value of the temperature coefficient can be adjusted easily by varying

TABLE I
TEMPERATURE-STABLE CA-V GARNET CHARACTERISTICS

PARAMETER	MEASURED VALUE	
$4\pi M_s$	420 G	(25°C)
Temp. Coef.	−0.07%/°C	(−20~20°C)
of $4\pi M_s$	−0.16	(0~20)
	−0.21	(20~40)
	−0.23	(20~60)
Tc	175°C	
ΔH	40 Oe	
ϵ	12.6	
tan δ_ϵ	2.5×10^{-4}	

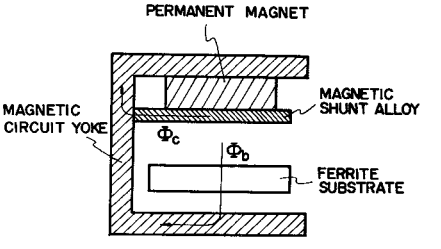

Fig. 11. Magnetic circuit for temperature compensation.

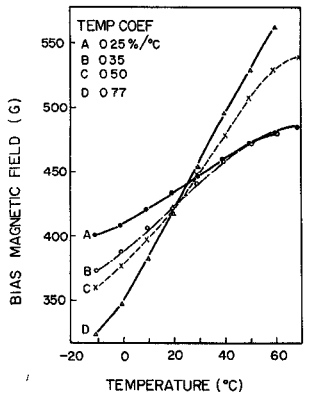

Fig. 12. Temperature variation on bias magnetic field.

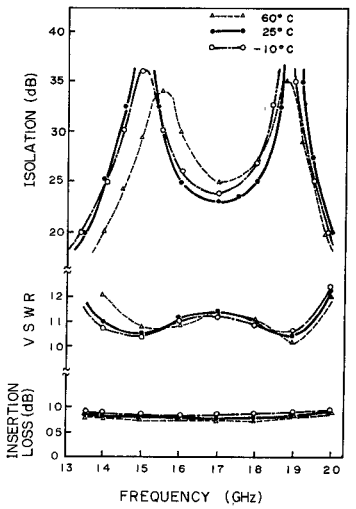

Fig. 13. Isolation, VSWR, and insertion loss of a temperature-stabilized double-tuned lumped-element circulator.

the plane size and thickness of the magnetic shunt alloy.

A 1.7-GHz band lumped-element circulator, temperature-stabilized with a bias magnetic field, has been successfully developed. Temperature dependences of various characteristics of the double-tuned circulator are shown in Figs. 13 and 14. In the ambient temperature range from −10°C to 60°C, a 20-dB isolation bandwidth of about 600 MHz (fractional bandwidth of about 35 percent), insertion loss of less than 0.95 dB with a ripple of less than 0.15 dB, and input/output VSWR of less than 1.22 have been obtained. It has been very difficult to get a 20-dB isolation bandwidth of more than 500 MHz at 60°C without the aid of a shunting alloy. The temperature coefficient 0.25 percent/°C of the magnetic field used and the frequency shift 0.04 percent/°C of the single-tuned junction part (calculated from the reactance variation at the center frequency shown in Fig. 14) correspond fairly well with each theoretical value predicted already.

Temperature dependence of various characteristics of the triple-tuned circulator temperature-stabilized in the same way, are shown in Figs. 15 and 16. In the temperature range from −10°C to 60°C, a 20-dB isolation bandwidth of more than 950 MHz is obtained. Figs. 14 and 16 make it clear, in addition, that in a broad-band circulator, the

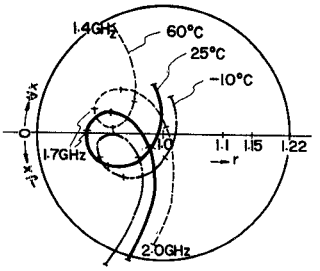

Fig. 14. Temperature variation on input impedance of a double-tuned circulator.

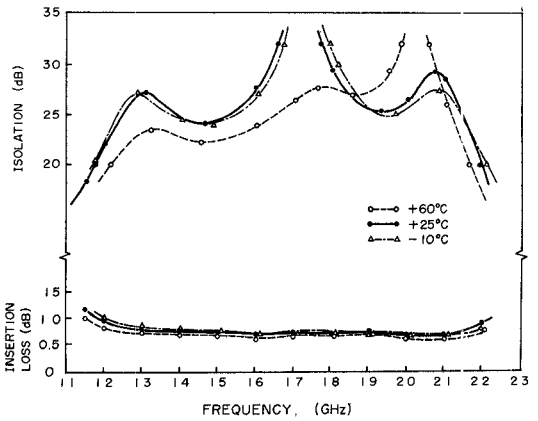

Fig. 15. Isolation and insertion loss of a temperature-stabilized triple-tuned lumped-element circulator.

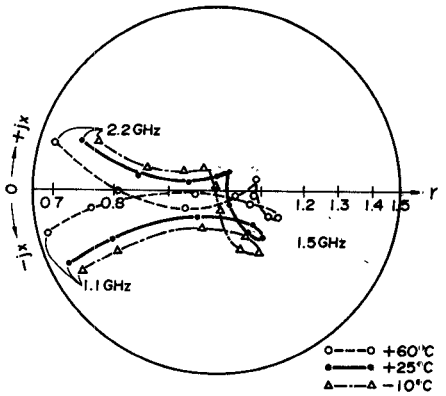

Fig. 16. Temperature variation on input impedance of a triple-tuned circulator.

discrepancy between center frequencies of the junction part and the wide-banding network should further be compensated for in order to achieve better temperature stabilization.

IV. CONCLUSION

In order to obtain a practical microwave lumped-element circulator, a design consideration for bandwidth broadening and temperature stabilization has been presented. Based on the results, a 1.7-GHz lumped-element circulator which is competitive with conventional distributed-constant circulators, has been developed.

By investigating eigeninductances of the circulator junction, the residual inductance of the in-phase excita-

tion and the distributed parallel capacitance have been specified, together with an actual nonreciprocal filling factor. A 1.7-GHz double-tuned and triple-tuned broad-band lumped-element circulator with a new type of integrated wide-banding network have been successfully fabricated. The network consists of three series resonant circuits which are formed on the back of the junction substrate in three-fold rotational symmetry.

A design theory for temperature compensation of the lumped-element circulator has been derived from circulator conditions. The design diagram presents the required compensating quantity of the bias magnetic fields, and the resultant variation of both the center frequency and the fractional bandwidth. Based on the results, temperature-stable broad-band lumped-element circulators have been developed, which guarantee 20-dB isolation bandwidths of 600 MHz (double-tuned type) and 950 MHz (triple-tuned type) throughout the temperature range of $-10°C \sim 60°C$.

APPENDIX

In the above resonance range where it can be assumed that $\sigma \gg 1$ and $h \gg 1$, (30)–(32) are simplified by using (25) and (26) as follows:

$$\frac{dH_{ex}}{H_{ex}} \approx \frac{1}{2}\frac{d(4\pi M_s)}{4\pi M_s} \tag{A-1}$$

$$\frac{df}{f} \approx -\frac{p}{2\sigma}\frac{dH_{ex}}{H_{ex}} \approx 0 \tag{A-2}$$

$$\frac{dw}{w} \approx -\frac{df}{f} \approx 0. \tag{A-3}$$

Thus, UHF or VHF circulators, which are usually biased at a strong magnetic field, are expected to be easily temperature-compensated by setting up the temperature coefficient of bias magnetic field to be one half of that of saturation magnetization. This method differs from the former [2], but (A-1) and (A-2) can be confirmed [15] by obtaining corresponding absolute value for H_{ex} and f against the variation of $4\pi M_s$ directly from the circulator conditions (18) and (19).

ACKNOWLEDGMENT

The author would like to thank Dr. Y. Konishi (Technical Research Labs., Japan Broadcasting Corporation) for his valuable discussion and guidance. The author would also like to thank Dr. T. Tsuji and H. Takamizawa for preparing the ferrite material, T. Itano for his help with experiments, Y. Akaiwa for valuable discussion, and Dr. K. Ayaki and Dr. K. Sekido for their encouragment and guidance.

REFERENCES

[1] R. H. Knerr, "A thin film lumped-element circulator," presented at *G-MTT Int. Microwave Symp.* (Dallas, Tex.), MPM-1-8, May 1969.
[2] Y. Konishi, "Lumped element Y circulator," *IEEE Trans. Microwave Theory Tech.* (*1965 Symp. Issue*), vol. MTT-13, pp. 852–864, Nov. 1965.
[3] R. H. Knerr, C. E. Barnes, and F. Bosch, "A compact broad-band thin-film lumped-element *L*-band circulator," *IEEE Trans. Microwave Theory Tech.* (*1970 Symp. Issue*), vol. MTT-18, pp. 1100–1108, Dec. 1970.
[4] R. H. Knerr, "An improved equivalent circuit for the thin-film lumped-element circulator," *IEEE Trans. Microwave Theory Tech.*, vol. MTT-20, pp. 446–452, July 1972.
[5] Y. Konishi and N. Hoshino, "Design of a new broad-band isolator," *IEEE Trans. Microwave Theory Tech.*, vol. MTT-19, pp. 260–269, Mar. 1971.
[6] Y. Konishi, "New theoretical concept for wide band gyromagnetic devices," *IEEE Trans. Magn.* (*1972 INTERMAG Conf.*), vol. MAG-8, pp. 505–508, Sept. 1972.
[7] I. Ikushima and M. Maeda, "A 1.7 GHz lumped-element circulator stable over a wide range of temperature," presented at *S-MTT Int. Microwave Symp.* (Atlanta, Ga., June 1974).
[8] J. Helszajn and M. McDermott, "The junction inductance of a lumped-constant circulator," *IEEE Trans. Microwave Theory Tech.* (Corresp.), vol. MTT-18, pp. 50–52, Jan. 1970.
[9] H. Katoh and T. Itano, "A 1.7 GHz-band integrated-circuit lumped-element circulator," in *Proc. 1972 Annu. Nat. Conv. Inst. Electron. Commun. Eng.* (Japan), no. 683, Apr. 1972.
[10] H. Katoh, "An integrated-circuit broad-band lumped-element circulator for the 1.7 GHz-band," *Trans. Inst. Electron. Commun. Eng.* (Japan), vol. 57-B, pp. 281–288, May 1974.
[11] R. A. Pucel and D. J. Massé, "Microstrip propagation on magnetic substrates—Part I: Design theory," *IEEE Trans. Microwave Theory Tech.*, vol. MTT-20, pp. 304–308, May 1972.
[12] Y. Konishi, "Propagation constant of strip-line loaded with arbitrarily magnetized ferrite," *Trans. Inst. Electron. Commun. Eng.* (Japan), vol. 54-B, pp. 30–38, Jan. 1971.
[13] H. Takamizawa, K.-I. Yotsuyanagi, and T. Inui, "Polycrystalline calcium–vanadium garnets with narrow ferrimagnetic resonance linewidth," *IEEE Trans. Magn.* (*1972 INTERMAG Conf.*), vol. MAG-8, pp. 446–449, Sept. 1972.
[14] Y. Akaiwa, "Input impedance of a circulator with an inphase eigen-excitation resonator," *Electron. Lett.*, vol. 9, no. 12, pp. 274–275, June 1973.
[15] H. Katoh, H. Takamizawa, and T. Itano, "Temperature stabilization of 1.7 GHz-band lumped-element circulator," Paper of Prof. Group on Microwave, *Inst. Electron. Commun. Eng.* (Japan), MW 74-7, Apr. 1974.